Cerebral Cortex March 2015;25:563–577
doi:10.1093/cercor/bht241
Advance Access publication September 22, 2013

FEATURE ARTICLE
Coding of Object Location in the Vibrissal Thalamocortical System

Chunxiu Yu[1], Guy Horev[2], Naama Rubin, Dori Derdikman, Sebastian Haidarliu and Ehud Ahissar

Department of Neurobiology, Weizmann Institute of Science, Rehovot 76100, Israel [1]Current address: Department of Psychology and Neuroscience, Center for Cognitive Neuroscience, Duke University, Durham, NC 27708, USA [2]Current address: Cold Spring Harbor Laboratory, Cold Spring Harbor, NY 11724, USA

Address correspondence to E. Ahissar, Department of Neurobiology, Weizmann Institute, Rehovot 76100, Israel. Email: ehud.ahissar@weizmann.ac.il

Chunxiu Yu and Guy Horev contributed equally to this work (co-first authors).

In whisking rodents, object location is encoded at the receptor level by a combination of motor and sensory related signals. Recoding of the encoded signals can result in various forms of internal representations. Here, we examined the coding schemes occurring at the first forebrain level that receives inputs necessary for generating such internal representations—the thalamocortical network. Single units were recorded in 8 thalamic and cortical stations in artificially whisking anesthetized rats. Neuronal representations of object location generated across these stations and expressed in response latency and magnitude were classified based on graded and binary coding schemes. Both graded and binary coding schemes occurred across the entire thalamocortical network, with a general tendency of graded-to-binary transformation from thalamus to cortex. Overall, 63% of the neurons of the thalamocortical network coded object position in their firing. Thalamocortical responses exhibited a slow dynamics during which the amount of coded information increased across 4–5 whisking cycles and then stabilized. Taken together, the results indicate that the thalamocortical network contains dynamic mechanisms that can converge over time on multiple coding schemes of object location, schemes which essentially transform temporal coding to rate coding and gradual to labeled-line coding.

Keywords: active sensing, anesthetized rats, artificial whisking, convergence dynamics, neuronal representations, touch

Introduction

Active vibrissal touch is mediated by a hierarchical array of parallel and nested motor-sensory loops (Fig. 1) (Kleinfeld et al. 2006; Bosman et al. 2011). The sensory part of this array conveys information encoded by whisker-object interactions (Szwed et al. 2003; Arabzadeh et al. 2005; Lottem and Azouz 2008; Ritt et al. 2008; Petersen et al. 2009) along at least 4 parallel pathways (Urbain and Deschenes 2007; Diamond et al. 2008). According to data accumulated so far, 2 of these pathways, the paralemniscal and extralemniscal, convey information required for decoding azimuthal object position (Knutsen and Ahissar 2009). The paralemniscal pathway conveys "Whisking" information (information on whisker movement regardless of contacts with external objects) via a rostral sector of the posterior complex of the thalamus (POm) (Sharp and Evans 1982; Yu et al. 2006; de Kock and Sakmann 2009). The extralemniscal pathway conveys "Touch" information (information derived from touch interactions with external objects) via the ventrolateral sector of the ventro-posterior-medial nucleus of the thalamus (VPMvl) (Pierret et al. 2000; Yu et al. 2006). The POm and VPMvl outputs converge in layers 4–6 of the secondary somatosensory cortex (S2) (Carvell and Simons 1987; Alloway et al. 2000; Pierret et al. 2000), and to a lesser degree in the primary somatosensory cortex (S1) (Pierret et al. 2000). Touch information combined with Whisking information (Whisking/Touch) is also conveyed to S1 by 2 lemniscal pathways (Urbain and Deschenes 2007; Diamond et al. 2008), passing through the "heads'" and "cores'" of VPM barreloids which together form what is termed here the dorso-medial part of VPM (VPMdm) (Yu et al. 2006).

Azimuthal object localization by whiskers most likely requires integration of Whisking and Touch signals (Szwed et al. 2003; Curtis and Kleinfeld 2009). Such interactions may occur already at the brainstem level (Furuta et al. 2008). Still, given that separated Whisking and Touch signals exist at the thalamic level (Yu et al. 2006), that rich interactions between pathways (Carvell and Simons 1987; Alloway et al. 2000; Pierret et al. 2000) and signals (Bureau et al. 2006; Crochet and Petersen 2006; Derdikman et al. 2006; Curtis and Kleinfeld 2009; de Kock and Sakmann 2009) occur within the thalamocortical network, that silencing S1 abolishes azimuthal object localization in mice (O'Connor, Clack et al. 2010), and that timed activation of S1 can replace Touch information for azimuthal localization (Venkatraman and Carmena 2011), the working hypothesis of this study was that meaningful internal representations of azimuthal object location are first generated in the thalamocortical network.

The vibrissal thalamocortical system is a highly connected and highly interactive network (Hoogland et al. 1987; White and Keller 1987; Agmon and Connors 1992; Deschenes et al. 1994; Bourassa et al. 1995; Gil et al. 1999; Swadlow 2000; Castro-Alamancos and Calcagnotto 2001; Ghazanfar and Nicolelis 2001; Alloway and Roy 2002; Guillery and Sherman 2002; Nicolelis and Fanselow 2002; Alloway et al. 2003; Bruno et al. 2003; Castro-Alamancos 2004; Bokor et al. 2005, 2008; Bruno and Sakmann 2006; Brecht 2007; Groh et al. 2008) embedded within a global motor-sensory closed loop (Fig. 1). In order to eliminate closed-loop effects induced by the global loop, the global loop must be artificially opened. Practically, the motor-sensory loop can be opened in several ways. In one common paradigm the animal is anesthetized and the whiskers are activated passively, thus breaking the muscle-whisker coupling (Fig. 1, "passive"). However, since passive touch activates both Whisking and Touch pathways indiscriminately (Szwed et al. 2003), this approach is not helpful for studying the integration of these 2 types of signals. Thus we employed an alternative approach, in which the animal is anesthetized, the facial motor nerve is cut, and whisking is induced artificially by electrically stimulating the peripheral branch of the motor nerve (Fig. 1, "active") (Zucker and Welker 1969). With this artificial whisking approach, the mechanics of active

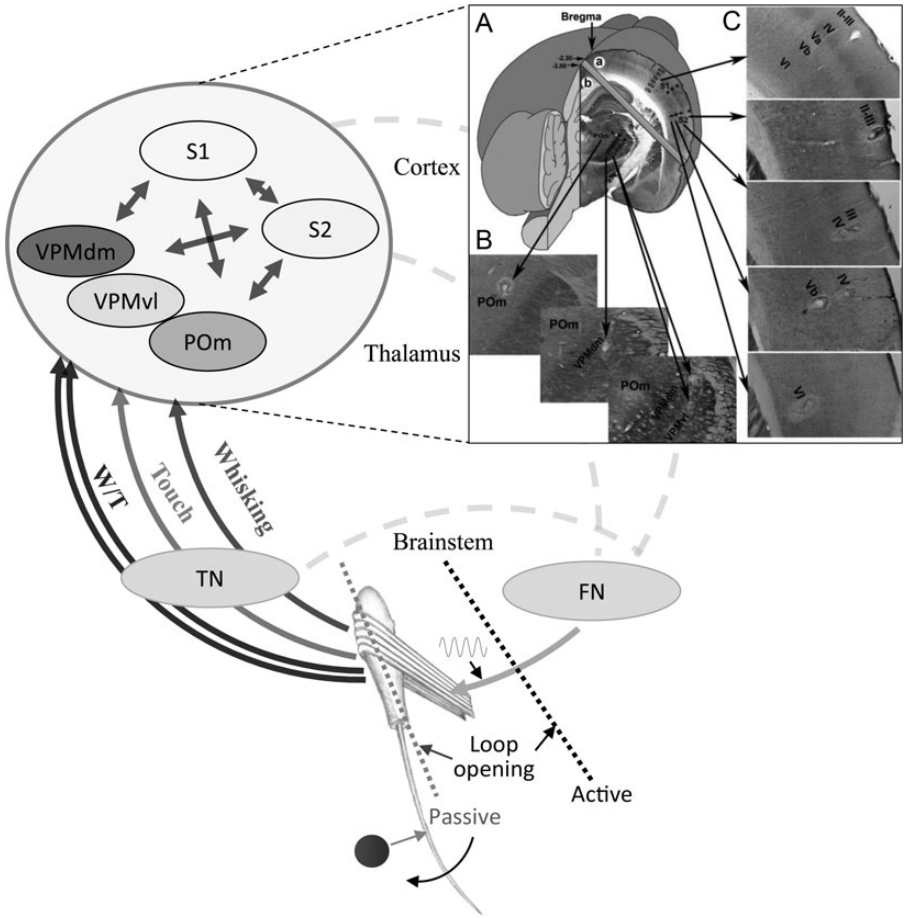

Figure 1. Working hypothesis and experimental design. Scheme of signals and neuronal stations involved in this study. Afferent signals that compose the working hypothesis for this study are (solid arcs) consist of Whisking signals (signals that contain information on whisker movement regardless of contact with external objects) that are carried by the paralemniscal pathway, Touch signals (signals that contain information on contact with external objects and no information on whisker motion) that are carried by the extralemniscal, and Whisking/Touch (W/T) signals (signals that contain information on both whisker movement and contact with external objects) that are carried by the 2 lemniscal pathways (Szwed et al. 2003; Yu et al. 2006). Dashed arcs represent collections of pathways and neuronal stations not relevant for this study (see Kleinfeld et al. 2006; Ahissar and Knutsen 2008). Two optional ways to open the motor-sensory loop are depicted. 1) Opening that preserves active touch (Black). The facial motor nerve is cut (black dashed line) and the muscles are activated electrically and move the whisker back and forth (black arrow arc) either in air or against an object. 2) Opening that does not preserve active touch (gray). By using passive touch (object moves the whisker, gray arrow), the loop is effectively opened because the coupling between muscle and whisker is broken (dashed gray line). FN, facial nucleus; TN, trigeminal nuclei; S1, primary somatosensory cortex; S2, secondary somatosensory cortex. Inset: Recording sites (indicated by asterisks) in the rat cortex and thalamus. (*A*) Schematic 3D image representing all the recording sites shown in 2 digital photomicrographs of a dorsolateral segment of a coronal slice about 2.30 mm caudal to bregma (a), and of a ventromedial segment of a coronal slice about 3.80 mm caudal to bregma (b). (*B*) Thalamic slices. (*C*) Cortical slices. Brain slices were stained for cytochrome oxidase. Asterisk with 2 arrowheads indicates recording sites in layers 4–6 in the S2. POm, posteromedial complex; S1, primary somatosensory cortex; S2, secondary somatosensory cortex; VPMdm and VPMvl, the dorsomedial and ventrolateral compartments, respectively, of the ventral posterior medial nucleus (VPM) of the thalamus.

touch, and thus, also receptor selectivity, can be preserved to a large extent (Zucker and Welker 1969; Szwed et al. 2003; Arabzadeh et al. 2005; Nguyen and Kleinfeld 2005; Derdikman et al. 2006; Yu et al. 2006; Ritt et al. 2008; Lottem and Azouz 2009). Importantly, as this approach involves anesthetized animals, whisking patterns, object contacts and recording sites are fully controlled by the experimenter.

Recent findings indicate that neurons in S1 of awake rats represent in their firing the azimuthal position of external objects (Curtis and Kleinfeld 2009; O'Connor, Peron et al. 2010), in a manner consistent with time-sensitive integration of whisking and touch signals (Curtis and Kleinfeld 2009). In the current work, we asked whether integrated position coding emerges in the cortex and whether additional representations exist in the thalamocortical network. Our artificial whisking paradigm revealed time-sensitive integration coding primarily in the VPM thalamus, layers 4–6 of S2 and layer 4 of S1; rate and temporal coding all across the thalamocortical network; and labeled-line (LL) coding in nonlemniscal and cortical layers as well as in the superficial layers of S1.

Materials and Methods

Animal Preparations and Recording Procedures

All procedures were approved by the Institutional Animal Care and Use Committee of The Weizmann Institute of Science. Adult male Albino Wistar rats ($n = 101$, 200–350 g) were used for this study; 19 rats for S2 recordings, 42 for S1 recordings and 40 for thalamic recordings. Other aspects of neuronal activity recorded in the thalamus and S1 were previously reported (Derdikman et al. 2006; Yu et al. 2006). The experimental protocols used were similar to those previously described (Szwed et al. 2003; Derdikman et al. 2006; Yu et al. 2006). In brief, surgery was performed under general anesthesia with urethane (1.5 g/kg, i.p.). Supplemental doses of anesthetic (10% of the initial dose) were administered when required. Atropine methyl nitrate (0.3 mg/kg, i.m.) was administered to prevent respiratory

complications. Anesthetized animals were mounted in a stereotaxic device (SR-6; Narishige; Japan), which allows free access to the somatosensory brain structures and whiskers. Body temprature was maintained at 37°C during experimental manipulations. A craniotomy was performed over the right thalamic or cortical stations according to known stereotaxic coordinates. During each recording, up to 4 tungsten microelectrodes (0.5–1 MΩ; Alpha Omega Engineering; Nazareth, Israel) were lowered in parallel until units drivable by manual whisker stimulations were encountered at the appropriate stereotaxic depth. Standard methods for single-unit recordings were used (Szwed et al. 2003). Single units were sorted online by spike templates (MSD-3.21; Alpha-Omega Engineering). Units were considered to be "single," that is, to represent individual neurons, only if their spike shapes were homogenous, and did not overlap with other units or noise, and if the units exhibited refractory periods of >1 ms in autocorrelation histograms. Artifacts produced by electrical stimulation were isolated by the online spike-sorter and removed from unit recordings.

Experimental Paradigms and Histology

A receptive field was defined for each recorded neuron as the set of whiskers that evoked a noticeable response to a manual passive deflection in any direction. Artificial whisking was induced as previously described (Szwed et al. 2003; Derdikman et al. 2006; Yu et al. 2006). Briefly, the facial nerve was cut, and its distal end mounted on a pair of silver electrodes. Bipolar, rectangular electrical pulses (0.5–4.0 V, 40 μs duration) were applied through an isolated pulse stimulator (Model 2100; A-M systems; Sequim, WA) at 83 or 200 Hz. Trials of 5 s were employed, each composed of a 2 s train of artificial whisking (5 Hz, 50% duty cycle) followed by a period of 3 s with no stimulation. Trials were employed in blocks of 12, 18, or 24 trials each. Blocks of artificial whisking in free air were interleaved with blocks of artificial whisking against an object positioned in front of an individual whisker within the receptive field of the neuron ("receptive whisker," RW). For each RW, a vertical pole (2 mm diameter) was placed at a distance away from the skin that was the equivalent of 70–90% of the whisker's length (from the skin surface to its tip), and at 3 different azimuthal positions (distanced 1–9 mm from the resting position of the whisker).

Each of the 4 whisking conditions (free-air and 3 object positions) was repeated in 2 blocks, interleaved in time. So as to mimic natural conditions, as much as possible, all whiskers of the mystacial pad were left intact throughout an experiment. Precautions were taken to insure and verify that the RW was the first whisker to contact the object during protraction. Thus, other whiskers located between the RW and the object were moved rostral to the object prior to each block of trials. Whisker movements were recorded at 1000 frames/s with a fast digital video camera (MotionScope PCI 1000; Redlake; San Diego, CA). Video recordings were synchronized with neurophysiological data with 1 ms accuracy (Szwed et al. 2003; Knutsen et al. 2005).

Typically, 4 electrodes were penetrated in parallel in each rat, of which neurons were typically recorded from 1–2 and from a single site per electrode. At the end of each recording session, electrolytic lesion was induced by passing currents (10 μA, 2 × 4 s, unipolar) through the tips of the recording electrodes. Rat brains were removed at the end of the recording session, fixed, sliced coronally and stained for cytochrome oxidase (CO). Using this technique, lesions located in the cortex and thalamus were clearly seen (Fig. 1). Only neurons for which the recording site was clearly evident were included in this study.

Analysis of Neuronal Data

Trajectories of whisker movements were analyzed offline, using semi-automatic whisker tracking that provided whisker angle and curvature at base (Knutsen et al. 2005). The time of whisking onset was determined from videos as the time at which the whiskers started moving. Raster plots and peristimulus time histograms (PSTHs; 1 ms bins, smoothed by convolution with a triangle of area 1 and a base of 10 ms) were computed and examined for all trains of each cell. Average response latencies (Lat50) were computed from the PSTHs as the delay from protraction onset to half peak response (Ahissar et al. 2000). Spike counts were the integrated number of spikes within a given time window, determined relative to the onset of protraction in each cycle. For SP calculations this window was 3–60 ms from protraction onset. For SPW calculations, the window was determined as the 40 ms following the initial nonselective response to whisking onset; the actual time windows were determined heuristically from the population response in each station (S1L23, 16–56 ms; S1L4, 13–53 ms; S1L5a, 24–64 ms; S2L23, 25–65 ms; S2L46, 20–60 ms; VPMdm, 13–53 ms, VPMvl, 10–50 ms, and POm 22–62 ms). Amplitudes of response peaks were calculated as the maximum of the smoothed PSTH. Statistical analysis was done with MATLAB (MathWorks, Natick, MA, USA).

The touch index (TI) was defined as:

$$\mathrm{TI} = \frac{(\mathrm{SP_T} - \mathrm{SP_W})}{(\mathrm{SP_T} + \mathrm{SP_W})}$$

where $\mathrm{SP_T}$ is the response (spike count/cycle) of a cell to whisking against an object during protraction, and $\mathrm{SP_W}$ is the response (spike count/cycle) of a cell to whisking in air during protraction. Thus, TI ~ 0 indicates pure whisking responses (i.e., responses to whisking that are not affected by the presence of an object), TI ~ 1 indicates pure touch responses, and TI ~−1 indicates complete responses suppression during object touch.

The adaptation index (AI) was defined as:

$$\mathrm{AI} = \frac{(\mathrm{SP} - \mathrm{SP_1})}{(\mathrm{SP} + \mathrm{SP_1})}$$

where SP is the spike count at a given cycle and $\mathrm{SP_1}$ is the spike count in the first cycle of the same condition (free air or touch). Thus, a positive AI indicates a facilitated response, and a negative AI a depressed response, relative to cycle 1.

The TI and AI 2 indices may produce unreliable values when firing rates are very low, summing in low denominator values. In our data, in only 7% and 8% of the cells, the denominator was <10 spikes and, in only 19% and 26%, it was <30 spikes for TI and AI, respectively.

Cluster Analysis of Cycles

Correlation coefficients (Pearson's R) were calculated between the |TI| or AI of each pair of cycles using all recorded cells ($n = 201$) as samples (Fig. 3*A*,*B*). The distance between each pair of cycles is defined as $1 - R$. Dendrogram plots of the cycles were generated by applying the Average Linkage Method to the matrix of distances between cycles (Statistics Toolbox; MATLAB).

Position Information Across Cycles

For dynamics of position coding (Fig. 6*A*,*B*), χ^2 was calculated for each individual cell in 9 pairs of consecutive cycles (1–2, 2–3, 3–4 … 9–10) using the Kruskal–Wallis test (statistical toolbox of MATLAB; MathWorks). For each response variable, the null hypothesis tested was "no difference between responses to different positions of the poles," where positions were P1, P2, P3, and no pole. The higher the χ^2 value, the higher the probability of rejecting the null hypothesis. Correction for multiplicity was performed using the false discovery rate (FDR) linear step-up procedure with $\alpha = 0.05$ (Benjamini and Hochberg 1995). After correction the cutoff P-value for significance of a single comparison was 0.0108 that is the equivalent to χ^2 value of 11 with 3 degrees of freedom. The correction, which was performed for 1809 comparisons (201 cells and 9 cycle pairs) in each coding scheme, provides a lower limit on the number of coding cells.

Position Information During Steady State

We used the Kruskal–Wallis test described above to assign one χ^2 value for the steady-state (SS) cycles (5–10). Cells that significantly distinguished between positions after correction for multiple comparisons were subjected to classification of coding schemes as defined below.

Classification of Coding Schemes

For each cell, we performed post hoc comparison between all pairs of positions (W-1, W-2, W-3, 1–2, 1–3, 2–3) using Tukey procedure for

confidence intervals (Benjamini et al. 2006) (MATLAB's multcompare). This procedure takes multiple comparisons into account and therefore controls the FDR of the entire analysis. Cells that did not pass the Kruskal–Wallis test, cells significant in Kruskal–Wallis but not significant in Tukey, and cells significant in both and for which all 3 positions differ from whisking but no difference between positions is evident, are considered noninformative (positionwise). The other cells were considered informative in the relevant response variable (see text and Table 1). For each variable, the coding class of a cell was exclusive so a cell was assigned only one class. However, an independent analysis was done for each variable; therefore, one cell could be informative in more than one variable and belong to different classes in different variables.

Bursting Analysis

We used the criterion of Sherman and coworkers (Ramcharan et al. 2005) for quantifying bursting levels: consequent spikes with interspike intervals ≤4 ms, and a preceding interval >100 ms, were all counted as burst spikes. We quantified bursting level as the percentage of all spikes that occurred during bursts within a given period (Burst%) (Ramcharan et al. 2005). This analysis was conducted for each unit separately in spontaneous and stimulation (artificial whisking) periods. ANOVA (anova1, MATLAB) was used for comparison between stations and Tukey's procedure for determining pairwise station differences in cases of significant ANOVA results. Bursting levels between spontaneous and artificial whisking periods in each station were compared using paired *t*-test (MATLAB) followed by FDR correction for multiple comparisons (Benjamini and Hochberg 1995).

Statistical Tests

Unless mentioned otherwise, all hypothesis tests were 2 tailed. We controlled the FDR to be lower than 5% either by using linear step-up procedure (Benjamini and Hochberg 1995) for multiple *t*-tests or by applying Tukey's procedure following ANOVA and Kruskal–Wallis (Benjamini et al. 2006).

Results

Single-unit activity was recorded, usually not simultaneously, in 8 thalamocortical stations during artificial active touch in anesthetized rats (see Materials and Methods section): 3 thalamic nuclei (VPMdm, $n = 30$; VPMvl, $n = 13$; POm, $n = 24$), and 3 S1 (S1L23, $n = 32$; S1L4, $n = 24$; S1L5a, $n = 23$) and 2 S2 (S2L23, $n = 33$; S2L46, $n = 22$) laminar divisions (Fig. 1, inset). Division to cortical stations was based on the patterning of afferent projections (Carvell and Simons 1987; Koralek et al. 1988; Chmielowska et al. 1989; Lu and Lin 1993; Alloway et al. 2000; Pierret et al. 2000). For each recorded cell, artificial whisking was induced in free air and against objects (vertical poles of 2 mm diameter) that were positioned at a radial distance equal to 70–90%

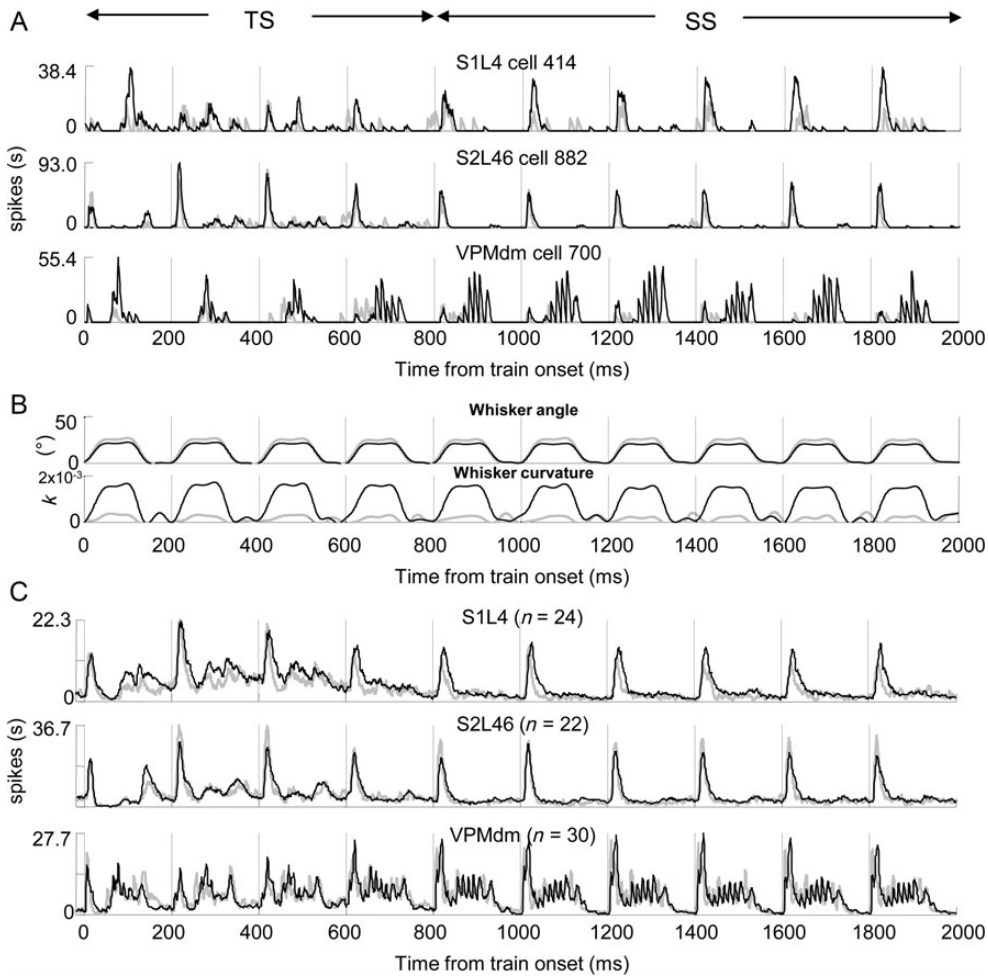

Figure 2. Dynamics of neuronal responses in example stations of the thalamus, S2 and S1. (*A*) PSTHs of individual neurons recorded in the thalamocortical network during free-air whisking (gray) and whisking against an object (black, averaged across all positions). Vertical lines indicate protraction onsets. (*B*) angular rotation (deg) and curvature (k) of a whisker (C1) recorded during one experiment. (*C*) Mean PSTHs of the entire population of neurons recorded in each of the 3 example thalamocortical stations (S1L4, S2L46, VPMdm) are depicted. Numbers of single units recorded and analyzed in each station are indicated in parentheses. Protraction onset times as in (*A*). TS, transient state; SS, steady state.

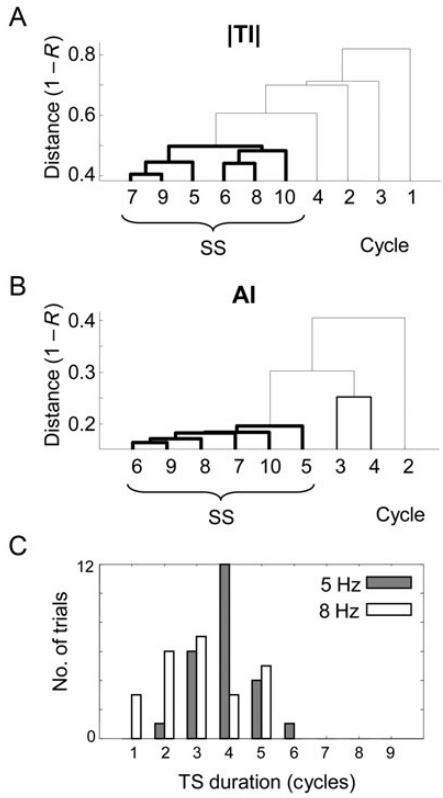

Figure 3. Dynamic grouping across levels and pathways. (*A* and *B*) Dendrograms of the correlation coefficients (Pearson's *R*) of |TI| (*A*) and AI during whisking in air (*B*) between cycles across the entire recorded thalamocortical population. The |TI|s and AIs were first computed for each individual neuron, and then correlated between each pair of cycles for the entire population ($n = 201$ neurons). Each node of a dendrogram represents a cycle. The height of the branches (along the *Y*-axis) represents the distance ($1 - R$) between its 2 associated leave nodes. Black thick lines indicate groups of nodes in the dendrogram where the linkage was less than the MATLAB default threshold (0.7 of max). (*C*) Distribution of TS duration (in cycles) in trials of whisking against objects ($n = 24$ trials) at 5 Hz ($n = 201$ neurons) and 8 Hz ($n = 71$ neurons) as determined by response patterns of all neurons recorded across the thalamocortical network. TS duration was determined by hierarchical clustering of the mean response in each station in each trial (see Materials and Methods section).

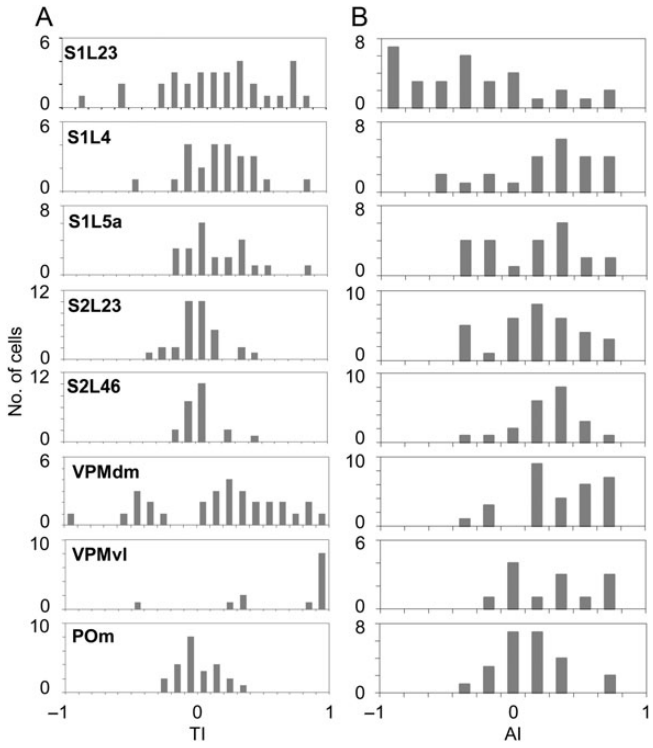

Figure 4. Distributions of touch indexes (TI) (*A*) and adaptation indexes (AI) during touch trials (*B*) at steady state. For each individual neuron, indexes were computed for their average responses during cycles 5–10. Touch responses were averaged across all positions.

of whisker length (inducing light touch) and in 1 of 3 azimuthal positions along the trajectory of the whisker: P1 (posterior), P2 (mid), and P3 (anterior) (see Materials and Methods section). Whisking was induced at 5 Hz with constant-amplitude bouts of 2 s (10 whisking cycles) interposed by 3 s intervals (Szwed et al. 2003). Whisking amplitude, which was constant during each experiment but varied across experiments due to interindividual and surgical variations, was $14.5 \pm 6.6°$ (mean ± SD) for the Whisking (in air) condition and $12.2 \pm 6.7°$ for Touch conditions.

Response Dynamics

The systematic application of a constant whisking pattern was used to reveal intrinsic response dynamics across the thalamocortical network. Neurons in the thalamocortical network were typically excited upon each protraction onset, both while whisking in air and while whisking against an object (Fig. 2*A*). The effect of light object touch on whisker angle trajectory (measured at the base of the whisker) was usually small, whereas its effect on whisker curvature (at the base) was large (Fig. 2*B*). The effect of object touch on neuronal responses varied from neuron to neuron, cycle to cycle, and one stimulation mode to another (Fig. 2*A*). Averaging of neuronal responses in each station reduced differences between stimulation modes (whisking in air and whisking against an object), while preserving variations between stations and cycles (Fig. 2*C*).

While response patterns of stations differed, the patterns exhibited similar general dynamics. In the first few cycles, neuronal responses exhibited clear cycle-to-cycle modulations, while during subsequent cycles, response patterns stabilized (Fig. 2). These modulations were not induced by modulations in the stimulation pattern which was constant across all cycles (Fig. 2*B*). In order to analyze cycle-by-cycle dynamics of response intensity, responses for each neuron in each cycle were quantified by integrating spike counts for the first 100 ms from protraction onset. The effects of object contact and response dynamics were quantified using a TI, which represents a normalized touch response, and an AI, which represents normalized dynamics of response intensity (see Materials and Methods section).

The dynamics of the magnitude of the modulations induced by touch, regardless of their sign, were examined by computing the absolute value of TI ($|TI|$) for each cell in each cycle. $|TI|$ was analyzed instead of TI in order to create a unipolar distinction between responses that are modulated ($|TI| \to 1$) and those that are not modulated ($|TI| \to 0$) by touch. AI was also computed for each cell in each cycle. The similarity of $|TI|$ and AI across cycles was examined by measuring Pearson's correlation coefficient (R) between cycles across all recorded cells ($n = 201$). Average link clustering of these correlation coefficients [dendrogram of the average distance ($1 - R$) between cycles; Fig. 3*A*,*B*] revealed that cycles 5–10 were highly correlated ($R_{|TI|} > 0.52$; $R_{AI} > 0.77$) with each other. The distribution of the correlation coefficients among cycles 5–10 was statistically different ($P << 0.001$, *t*-test) than

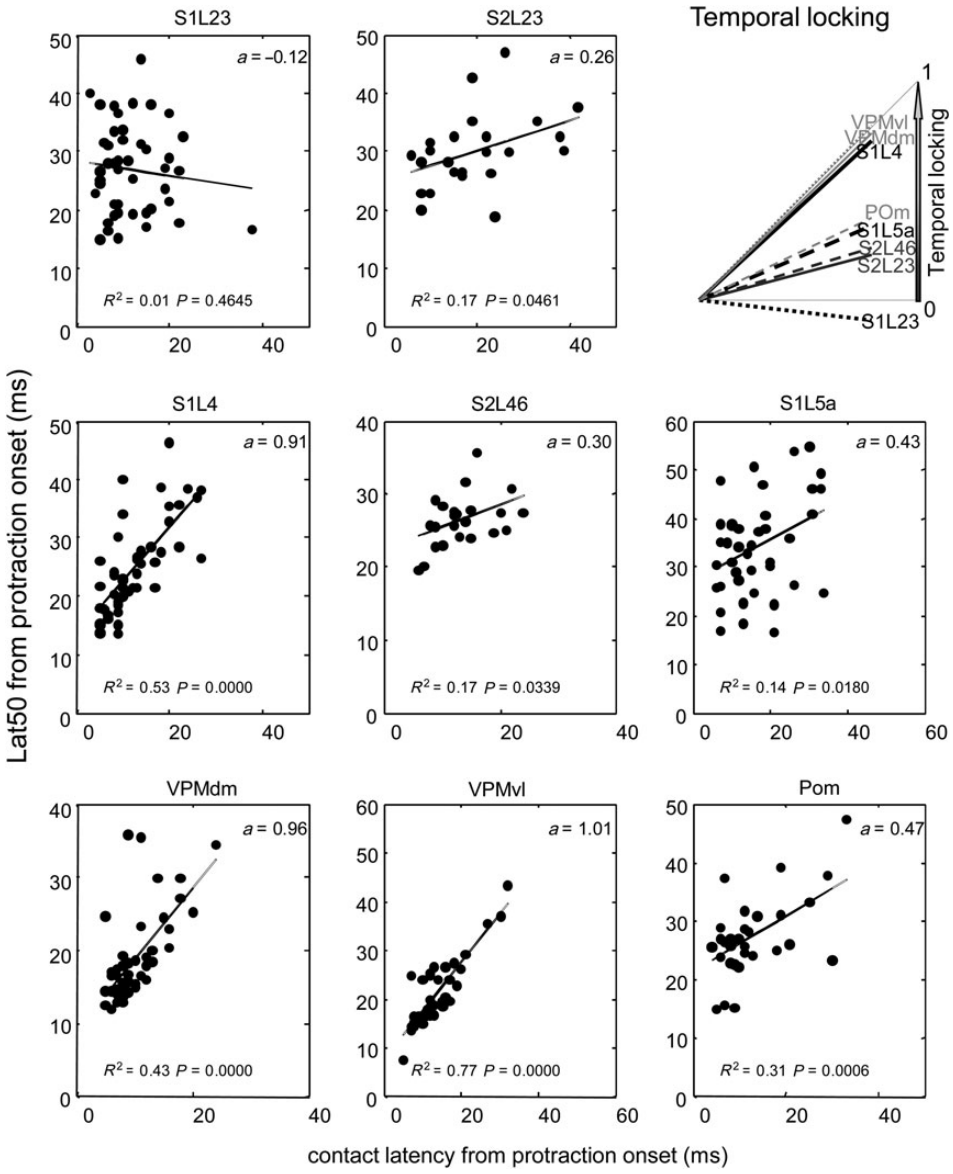

Figure 5. Temporal locking in each station during the SS. Each dot represents one neuron in one object position, and its coordinates represent contact latency (abscissa) and response onset latency (ordinate, lat50) from protraction onset. Dots with the same coordinates hide each other. All linear regression lines are depicted again in the inset, where slope = 0 means no temporal locking and slope = 1 means perfect temporal locking.

those among cycles 1–4. Conducting the same analysis with TI instead of |TI| yielded similar results ($R_{TI} > 0.55$). Given the observed difference between the first (cycles 1–4) and subsequent (cycles 5–10) whisking cycles, we analyzed them separately. The first (cycles 1–4) are referred to as transient-state (TS) cycles, and cycles 5–10 as SS cycles. This article focuses on the SS responses.

Transient and Steady States

In order to analyze the variability of TS duration across trials, the duration of TS was calculated for each single trial in an artificial whisking block ($n = 24$ trials) using the same clustering method presented above. The distributions of TS durations showed that the thalamocortical network stabilized its spike-count pattern within 3.9 ± 0.9 cycles and 3.0 ± 1.3 for 5 and 8 Hz bouts, respectively (Fig. 3*C*).

The distributions of SS TIs of individual neurons across all 8 stations tested are depicted in Figure 4*A*. As previously described (Yu et al. 2006), we observed that, in the thalamus, POm neurons mainly exhibit pure whisking responses with a TI around 0 (median of −0.02), VPMvl neurons mainly display pure touch responses with a TI around 1 (median of 0.91), whereas VPMdm neurons display a bimodal distribution with TIs either greater or less than 0 (with medians of 0.39 and −0.47, respectively). In contrast, neurons in S1L23 exhibited a broad distribution with $-1 < TI < 1$ (median of 0.20). S1L4 and S1L5a neurons displayed a narrower distribution, with medians of 0.20 and 0.09, respectively. The TIs of neurons in S2L23 and S2L46 were distributed mainly around TI = 0, with medians of 0.00 and 0.03, respectively, which resembled the distribution of TIs for neurons in the POm. This similarity, together with a consistent distribution of anatomical projections (Carvell and Simons

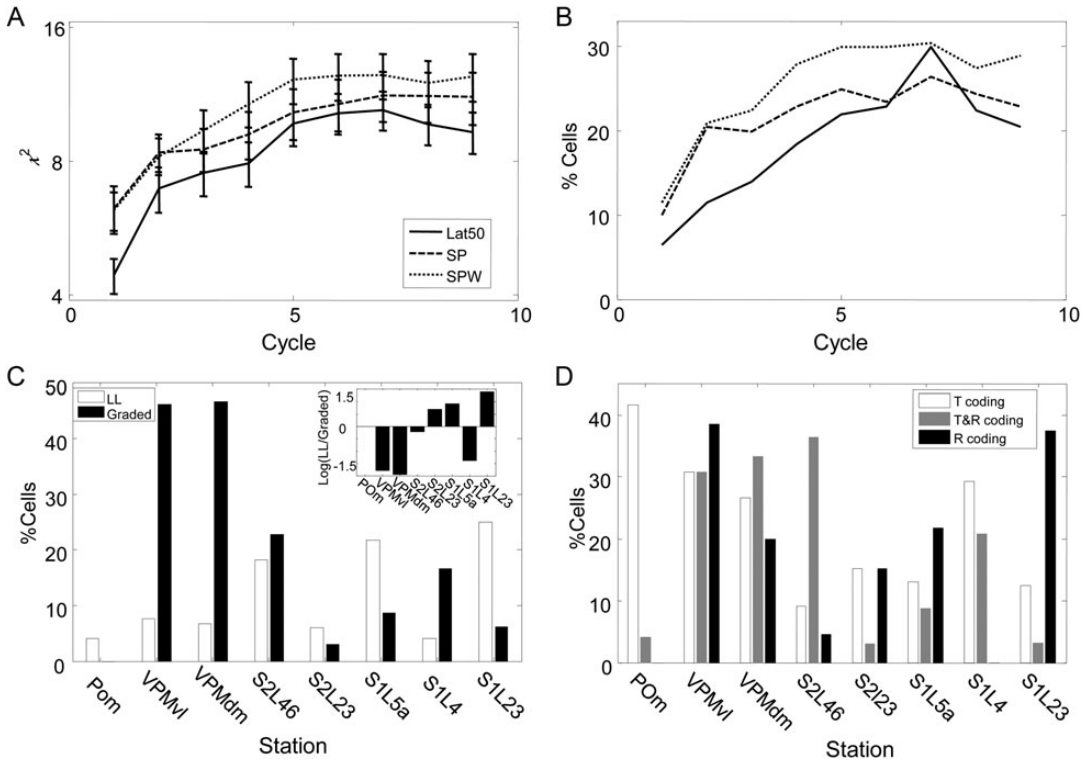

Figure 6. Position coding in the thalamocortical network. (*A*), Position selectivity represented by χ^2-values (average ± SEM, $N = 201$ neurons) from Kruskal–Wallis (KW) test, (see Materials and Methods section) presented versus cycle number for latency (Lat50), spike count (SP) and windowed spike count (SPW) used to evaluate thalamocortical location information. The higher the χ^2-value the higher the position selectivity is. (*B*) A lower bound on the fraction of cells in the thalamocortical network that exhibited a significant difference in the KW test (after FDR correction for multiplicity; $\alpha = 0.05$) between responses to different pole positions. (*C*) Distribution in the 8 different stations of the LL and graded codes resulting from the classification algorithm in SP. Inset, Log of the ratio between the fractions of LL and graded significant coding cells. (*D*) Distribution of cells that code only in time (lat50; T coding) only in rate (SP; R coding) or in both (T&R coding).

Table 1
Code classification summary across the entire thalamocortical network

Coding scheme		Lat50 Mean χ^2	Lat50 % cells	SP Mean χ^2	SP % cells	SPW Mean χ^2	SPW % cells
Noninformative		5.4	62.7	4.6	67.1	4.4	55.7
Labeled line	LL	26.8	15.9	20.1	11.9	18.1	18.9
Monotonic increasing	Inc	35.7	8.9	59.8	4.5	66.7	6.5
Monotonic decreasing	Dec	27	4	44.7	6.5	65.4	8
Nonmonotonic	NM	44.7	5	47.9	6	44.7	7.4
Other		14.4	3.5	14.3	4	14.3	3.5

1987; Alloway et al. 2000), suggests that S2 neurons are driven primarily by paralemniscal inputs.

The distributions of SS AIs across the recorded stations (AIs during touch trials are depicted in Fig. 4*B*; AIs during whisking in air showed a similar trend) indicate that most neurons were facilitated (AI > 0) during artificial whisking trains. Exceptions to this facilitation occurred with most of S1L23 neurons, and a small fraction of neurons in the other stations, which exhibited noticeable depression.

Touch neurons in the trigeminal ganglion exhibit high degree of temporal locking to contact, that is, firing at a constant delay after contact onset, while whisking neurons do not (Szwed et al. 2003). We computed the temporal locking to contact of all recorded thalamocortical neurons. These neurons exhibited a variable degree of temporal locking, which was strongly dependent on their station: Neurons in thalamic and cortical lemniscal and extralemniscal stations (VPMdm, VPMvl, S1L4) exhibited high degree of locking, whereas paralemniscal neurons (POm, S1L5a, S2L23, S2L46) exhibited poor temporal locking. S1L23 neurons did not exhibit any temporal locking as a population (Fig. 5).

Multiple Thalamocortical Coding Schemes

We considered information that is available to potential readout circuits in the brain and coded in 1 of 3 common response variables: response onset time, quantified by the latency to half peak of the PSTH (Lat50); mean response magnitude (rate), quantified as the mean spike count during a single whisker protraction (SP); windowed response magnitude (rate), quantified as the mean spike count during a station-specific response window within a single whisker protraction (SPW, see Materials and Methods section for window times). Faithful to availability to neuronal readout circuits, we did not subtract spontaneous activity levels or responses to whisking

in air from the recorded responses and did not limit the analysis to neurons whose responses passed certain a priori criteria (e.g., response strength), assuming that the operation of a given circuit in the brain is affected by the entire activity of all its neurons and inputs and not only by the activity of a selected subgroup or activity level.

We first analyzed the dynamics of position information across the thalamocortical network. The amount of information was assessed by computing the χ^2 value of the null hypothesis that there was no difference between responses to different positions of the poles; the higher the χ^2 value, the higher the probability of rejecting this null hypothesis. Cycle-by-cycle analysis of this relative position information (see Materials and Methods section) shows that, on average, the amount of position information conveyed by individual neurons across the thalamocortical network increased monotonically during the first 5 cycles, and stabilized during the SS cycles for each of the 3 basic response variables (Fig. 6*A*). The fraction of cells in the thalamocortical network that exhibited significant amount of position information in each of these codes increased from cycle to cycle, with a similar dynamics (Fig. 6*B*). This analysis thus reveals a saturation behavior of thalamocortical information toward a certain asymptotic level. During the SS, 63% (127 of 201) of the neurons carried significant ($P < 0.01$ after FDR correction for multiple comparisons, see Materials and Methods section) position information: 37% (75 of 201) in Lat50, 33% (66 of 201) in SP, and 44% (89 of 201) in SPW; 56 neurons carried both SP and SPW information, 45 both SPW and Lat50, and 32 both SP and Lat50.

Next, we examined the specific coding schemes by which thalamocortical information could be carried. Possible schemes can be categorized in 5 classes (Table 1): Noninformative (Non); Labeled line (LL), signaling one and only one position; Monotonic increasing (Inc), the response variable monotonically increased with azimuthal angle; Monotonic decreasing (Dec), the response variable monotonically decreased with azimuthal angle; Nonmonotonic (NM), the response variable did not change monotonically with azimuthal angle. We analyzed the information carried by each of the coding neurons in each response variable and in each possible coding scheme. Three of the coding schemes (Inc, Dec, and NM) were based on graded codes, in which the actual value of the variable was informative, and one (LL) was based on a binary code, in which information was carried by firing versus nonfiring. For each of the 3 variables, graded position codes contained more information on object position than the binary LL code. In contrast, for each variable, the LL code was exhibited by more neurons than any of the graded codes (Table 1).

Graded and binary codes distributed differently across stations of the thalamocortical network. For the SP variable, graded codes were most abundant in the VPM stations and the LL code was most abundant in cortical stations (Fig. 6*C*). In fact, the difference between the density of graded and binary coding cells in each station reveals a clear transformation from the VPM stations to 3 cortical domains: S2L23, S1L5a, and S1L23 (Fig. 6*C* inset). Notably, S1L4 exhibited a VPM-like distribution of coding cells. S2L46 contained a relatively high fraction of both graded and binary coding cells. Analysis of the SPW variable yielded similar results (not shown).

We further analyzed the distribution of time and rate coding (integrated over graded and binary codes) across the thalamocortical network. Neurons exhibiting only temporal (lat50) coding were more abundant in thalamic nuclei compared with cortical stations, whereas the distribution of neurons coding only by rate (SP) was comparable between thalamus and cortex (Fig. 6*D*). Neurons coding by both time and rate (T&R coding cells) were mostly abundant in 2 cortical stations (S1L4 and S2L46) and in VPM thalamic stations.

The various coding schemes were realized by different neurons in various manners, as demonstrated by the PSTHs computed for the SS responses (see examples in Fig. 7). Temporal coding cells exhibited PSTH peaks that were locked to contact times (Fig. 7*A*). Monotonic increasing and decreasing rate coding involved PSTH peaks typically at a constant latency from protraction onset and at magnitudes that increased or decreased with more anterior object positions, respectively (Fig. 7*B, C*). Interestingly, during the SS, many of the rate coding cells exhibited informative response early in the whisking cycle, even before contact occurred (Fig. 7*B–D*). This may indicate closed-loop or history-dependent processing, which can generate predictions regarding the next coming sensory input based on the previous cycle(s) (Ahissar 1998; Ahissar et al. 2000; Szwed et al. 2003; Golomb et al. 2006). The Inc and NM codes did not directly reflect magnitude coding at the periphery, as whisker curvatures and thus torques (Quist and Hartmann 2012) typically decrease with the azimuthal angle of contact (Bagdasarian et al. 2013). Windowed LL coding cells exhibited binary firing for a single position following their initial response component (Fig. 7*E*) whereas LL coding cells fired for only one position during protraction (Fig. 7*F*). Typically, LL coding neurons responded at lower rates than all other coding cells (34.2 ± 31.7 vs. 58.7 ± 40.6 spikes/s, peak response rates; $P = 0.013$, *t*-test), suggesting an inhibition-based mechanism. T&R coding cells exhibited rate coding combined with temporal locking to contact times (Fig. 7*G*).

Convergence Dynamics Across Time and Pathways

The coding schemes presented above are those schemes on which the thalamocortical network converged during the TS. The spatiotemporal dynamics of convergence was studied by analyzing the sequence of responses in different stations in relation to their 1) level affiliation (thalamic [VPMdm, VPMvl, and POm], cortical-input [S1L4, S1L5a, S2L23, and S2L46], and cortical-higher [S1L23]) and 2) pathway affiliation (lemniscal [VPMdm and S1L4], paralemniscal [POm, S1L5a, S2L23, and S2L46], and extralemniscal [VPMvl]). The dynamics of level relations (thalamus vs. cortex-input, Δ_levels) and pathway relations (lemniscal vs. paralemniscal, Δ_pathways) along the whisking train while whisking against objects are depicted in Figure 8*A,B*. The difference between the $|\mathrm{TI}|$s of the lemniscal and paralemniscal pathways was significantly different from 0 (*, $P < 0.05$, *t*-test) or highly significant (**, $P < 0.01$) throughout the whisking train (Fig. 8*A*, black). In contrast, the difference between the $|\mathrm{TI}|$s of the thalamus and cortex was (highly) significant ($P < 0.01$) only during cycles 2 and 3 (Fig. 8*A*, gray). The analysis of the AI revealed a significant difference only between the thalamic and cortical levels and only during cycles 2 and 3 ($P < 0.01$) (Fig. 8*B*). Thus, a general transition from a primarily level-dependent behavior to a primarily pathway-dependent behavior accompanied the TS to SS transition.

The spatiotemporal dynamics of the responses were studied in 2 major time scales: within and across whisking cycles.

Response order across thalamocortical stations within each cycle did not change between the TS and the SS, as shown by comparing cumulative distributions of response onset latencies (Fig. 8*C*,*D*). The 2 VPM nuclei were the first to respond, followed by activation of all other stations of which S1L23 and POm neurons tended to respond last. In contrast, the dynamics of the responses across cycles showed an inverse order: The peak of the low-pass filtered population response occurred first in the POm and S1L23, later in the other cortical stations and lastly in the 2 VPM stations (Fig. 8*E*), exhibiting a strong inversed correlation with the within-cycle latencies ($R^2 = 0.85$, $P = 0.001$).

Firing Mode of Thalamic Neurons

We quantified bursting levels by calculating the percentage of spikes which were part of a burst (Burst%; see Materials and Methods section). Average Burst% values in thalamic nuclei of awake visually fixating monkeys vary between 0.4 and 26.9 (Ramcharan et al. 2005). The average spontaneous Burst% values in the thalamic stations in our study were 4.4 ± 0.8, 10.1 ± 2.8, and $12.7 \pm 1.9\%$ in the POm, VPMvl, and VPMdm, respectively. VPM Burst% values differed significantly from POm and cortical (2.2 ± 0.4 across all cortical station) values ($P < 0.001$, ANOVA; 95% confidence interval, Tukey's procedure). During artificial whisking, Burst% values were 4.5 ± 0.7, 11.3 ± 1.7, and $7.5 \pm 1.2\%$, respectively (mean ± SEM; $P > 0.056$, *t*-test followed by correction for multiple comparisons).

Discussion

The repertoire of coding schemes for object location available at the vibrissal thalamocortical network was investigated using artificial whisking in anesthetized rats. We found that the thalamocortical network can represent object location using both graded and binary (LL) coding schemes applied to at least 3 response variables (latency, spike count, and windowed spike count). Each of these codes provides significant information on object location and thus can in principle guide motor-sensory behavior in behaving rats. This study thus suggests that a behaving rat can select among several coding schemes depending on the context, conditions, and brain state. There is no single code that must be used in all conditions. In the anesthetized rats, the dynamics of thalamocortical representations exhibited a convergence pattern, during which information on object position gradually increased (in all coding schemes) during a few whisking cycles and then stabilized—dynamics that may be relevant to behavioral dynamics of perception (Horev et al. 2011; Saig et al. 2012).

Dynamics of Thalamocortical Coding

Changes in response magnitudes and latencies during repeating sensory stimulations are common. Typically, with passive stimulations, these dynamics are classified as adaptation processes in which responses are gradually attenuated until stabilized (e.g., Ahissar et al. 1998; Ahissar et al. 2001; Ego-Stengel et al. 2001; Sosnik et al. 2001; Wang et al. 2010); such dynamics were shown to maintain information transfer in the vibrissal system (Maravall et al. 2007; Bale and Petersen 2009; Adibi et al. 2013). Here we describe, with artificial active sensing, dynamic changes that contain both reductions and increases in response magnitude (Figs 2 and 4). Interestingly, these dynamics were associated with an increase in the information on object position carried by the neurons (Fig. 6). One possible interpretation of these dynamics is that they are signatures of a thalamocortical convergence process, during which internal representations are formed (e.g., Hopfield 1982; Edelman 1993; Tweed 2003; Chakrabarti and Basu 2008; Wang et al. 2010) among the neurons composing the thalamocortical network. Importantly, although the details of the representations that emerged in our experiments depended on the sensory input, the dynamics of their formation, generally speaking, did not; it took 3–5 cycles to stabilize regardless of object existence or position. Moreover, this process was accompanied by slow dynamics of response magnitude, whose time scale was similar to code stabilization and whose order between stations was inversed to the order occurring in each cycle (Fig. 8). The co-existence of these fast and slow dynamics may reflect a co-existence of bottom-up and top-down processes (Fig. 9). If this is the case, then the weak slow activation of the POm before S1L23 may reflect motor-related priming of the top-down process.

These dynamics appear to be hard-wired in the thalamocortical system, since they can be triggered in an anesthetized rat and their pattern is generally constant. Thus, they may be triggered upon any significant change in the sensory input or top-down signals. With behaving rodents, for example, these dynamics may appear both upon whisking onset and upon the first contact with an object. Such an interpretation is consistent with our previous observation that, at least in some contexts, the number of contacting whisking cycles remains constant (around 4 contacts) and does not depend on task difficulty (Knutsen et al. 2006). According to this interpretation, although in the behaving rat additional closed-loop processes control the dynamics of the vibrissal system (Nguyen and Kleinfeld 2005; Towal and Hartmann 2006; Mitchinson et al. 2007; Diamond et al. 2008; Deutsch et al. 2012), thalamocortical hard-wired dynamics is still effective. If this is the case, the choice whether to wait for full thalamocortical convergence or not should depend on behavioral parameters such as criticality of perceptual acuity and competing behavioral drives.

Multiplicity of Coding Schemes and Thalamocortical Transformations

The multiplicity of coding schemes revealed may reflect the gradual evolution of more and more accurate mechanisms for object localization. We postulate that newer mechanisms build upon older ones and actually use the outputs of the latter during online processing. In fact, some of the codes described here can be transformed between each other by previously described mechanisms. For example, whisking and touch coding neurons (Yu et al. 2006) can interact via phase detection (Jeffress 1948; Ahissar 1998; Szwed et al. 2003; Curtis and Kleinfeld 2009; Groh et al. 2013) to yield T&R codes, and T&R codes can be transformed to LL codes via an inhibition-based threshold operation that lets through only the strongest signals. According to recent findings, this chain of transformations appears to be implemented by phase detection in S1L4 and S1L5a (Curtis and Kleinfeld 2009) or POm (Groh et al. 2013), projection of their outputs to S1L23 (Feldmeyer et al. 2002; Bureau et al. 2006; Schubert et al. 2007), and high activation thresholds of S1L23 neurons (Brecht 2007; Crochet et al. 2011) via strong local inhibition (Okun and Lampl 2008; Helmstaedter et al. 2009; Gentet et al. 2010; Crochet et al. 2011), consistent with the low firing

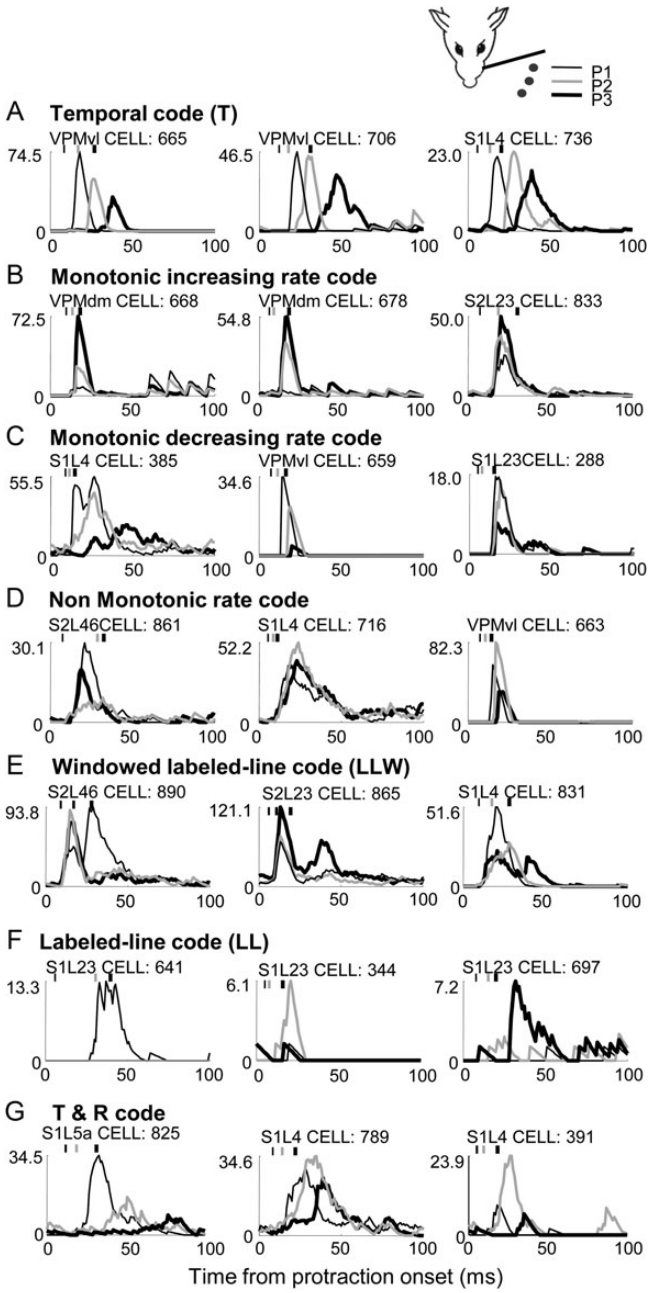

Figure 7. Examples of neurons coding azimuthal object location, grouped by coding schemes (3 examples in each). The line-styles of the PSTHs are coded according to object position (inset): p1 (most posterior, thin black), p2 (thick gray), and p3 (most anterior, thick black). Short vertical bars in each panel represent contact times, gray coded by position.

rate of our LL coding neurons (Fig. 7*F*). Thus, it appears that the iterative dynamics between thalamocortical stations converges to a SS in which graded coding at the thalamus is transformed to more LL coding in the (mostly supragranular) cortex (Fig. 6), via T&R coding that is shared between lemniscal thalamus and (mostly infragranular) cortex (Fig. 9).

In another path, whisking and touch coding neurons could interact via phase-locked loops (PLL, Ahissar 1998; Ahissar et al. 2000; Szwed et al. 2003) or $GABA_B$ inhibition (Golomb et al. 2006) to generate graded rate codes. These mechanisms are consistent with the response pattern during the SS in which many of the rate code representations actually predicted the occurrence of contact in their coded position (Fig. 6*B–D*), which indicates such closed-loop or history-dependent processing.

Possible Effects of Anesthesia and Artificial Whisking

Brains modulate their operational conditions across a wide spectrum of states that correspond to various behavioral modes (e.g., sleeping, waiting, exploring, palpating, localizing, identifying, attending, alerting, and grooming). Reductionist science, by definition, reduces the tested system by eliminating a large portion of its possible states. Accordingly, experimental neuroscience always involves elimination of a large portion of behavioral modes and brain states. The cost is that the relevance of neuronal activity recorded in one brain state to brain operation in another state is not obvious. In the current case, the relevance of our results, obtained with artificial whisking under urethane anesthesia, to neuronal mechanisms that operate during object localization in the behaving rodent depends on the effects of anesthesia and artificial whisking on neuronal responses, both in the periphery where external information is encoded and in the thalamocortical network.

So far, first-order vibrissal neurons appear to be barely affected directly by brain states, including anesthesia (Angel and Unwin 1970; Maggi and Meli 1986). However, these neurons might be affected via effects on whisker-follicle mechanics and whisking dynamics (Mitchinson et al. 2004, 2007; Birdwell et al. 2007; Hill et al. 2008; Ritt et al. 2008; Stuttgen et al. 2008; Towal and Hartmann 2008; Chiel et al. 2009; Simony et al. 2010). The major differences between artificial and natural whisking, with respect to their mechanics and dynamics, are in the blood supply to the follicle (Gottschaldt et al. 1973; Fundin et al. 1997), lack of active retraction (Berg and Kleinfeld 2003), a constant protraction profile and occasionally addition of small periodic "pumps" to the main protraction trajectory that are locked to the times of nerve activation (Szwed et al. 2003). However, these differences, which may affect details of neuronal responses, such as locking of spikes to times of onsets of artificial pumps, are not expected to affect principles of neuronal coding, such as, selectivity to whisking and touch. Studying neuronal selectivity in freely moving animals is extremely difficult due to limited traceability and control of animal behavior, internal modes, whisker movement, whisker contacts, single-unit separation, and exact sites of neuronal recordings. When tested in freely moving rats, neuronal activity in the trigeminal ganglion exhibited a wide distribution of selectivity to whisking and massive touch (Leiser and Moxon 2007). Yet, while the exact selectivity of individual first-order afferents to light touch in the awake rat is not yet clear, so far data are consistent with sensory afferents conveying differential Whisking and Touch signals, as demonstrated in anesthetized rats (Diamond et al. 2008).

Importantly, artificial whisking induces mechanical interactions between whiskers and objects that are similar to those induced by rats performing an object localization task. Angle protraction and absorption, and global and base curvatures of the contacting whiskers are within similar ranges in both conditions, as well as in head-fixed untrained rats (Bagdasarian et al. 2013). This further supports the assumption that peripheral inputs during artificial whisking are in the same range of magnitudes as during behavior.

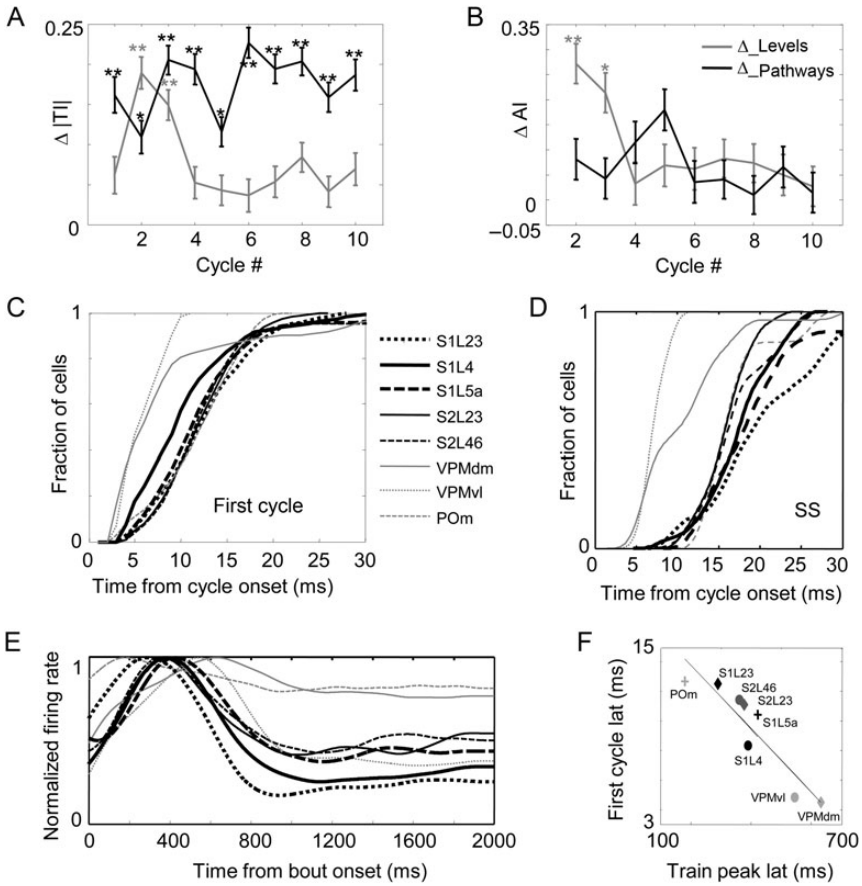

Figure 8. Dynamics of thalamocortical responses. (*A* and *B*) Dynamics of differences between the thalamus (VPMdm, POm) and cortex-input stations (S1L4, S1L5A, S2L23, S2L46) (Δ_levels; thalamus–cortex), and between the lemniscal (VPMdm, S1L4) and paralemniscal (POm, S1L5A, S2L23, S2L46) pathways (Δ_pathways; lemniscal–paralemniscal) for the |TI| (*A*) and AI (*B*). Δ depicts the difference (mean ± SEM) between |TI| or AI calculated for individual neurons in different levels (gray) or pathways (black). Significance levels were computed for the difference of each value of Δ from 0: *, $0.01 < P < 0.05$; **, $P < 0.01$. (*C* and *D*) Cumulative distributions of lat50 in each station during the first cycle (C) and SS (D). (*E*) Low-frequency (low-pass, cutoff frequency of 2 Hz, third-order Butterworth filter) component of the mean response of the entire recorded neuronal population in each station, depicted for all stations. (*F*) Relations between the within-cycle (median of lat50 in each station) and across cycles (latency to the peak of the low-frequency component in each station) in free air.

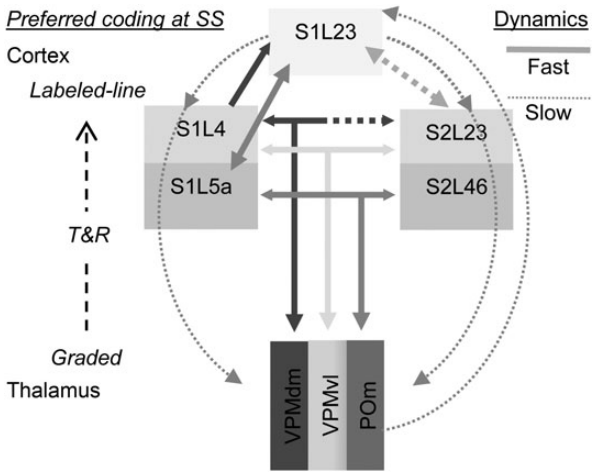

Figure 9. Summary of response dynamics in the thalamocortical network. Thalamic nuclei drive deep cortical layers which in turn drive S1L23 with fast dynamics on each whisking cycle. Slow response dynamics appears to flow in the reverse direction, from S1L23 to deep cortical layers to thalamus, where POm appears to lead this slow dynamics. Solid heavy arrows indicate known anatomical connections; dotted heavy arrows indicate suspected pathways; dotted light arrows indicate implied pathways.

Central neurons are affected significantly by anesthesia, as well as by other changes in brain states (Angel et al. 1973; Worgotter et al. 1998; Fanselow and Nicolelis 1999; Castro-Alamancos 2002; Greenberg et al. 2008; Lee et al. 2008; Poulet and Petersen 2008; Curto et al. 2009; Crochet et al. 2011). Mostly relevant to this study is the shift of thalamic neurons from a bursting mode under anesthesia to a tonic mode in alert behavior (McCormick and von Krosigk 1992; Sherman and Guillery 1996; Castro-Alamancos 2002). The level of bursting in our VPM neurons (but interestingly not POm neurons) was indeed higher than the level observed in the VP nuclei of awake monkeys (Ramcharan et al. 2005). Interestingly, induction of artificial whisking decreased the level of bursting in VPMdm, suggesting a partial shift to a tonic mode; such a shift could be induced via corticothalamic activation of metabotropic glutamate receptors (McCormick and von Krosigk 1992; Sherman and Guillery 1996; see Sosnik et al. 2001).

While magnitudes and correlations of cortical neuronal activity are significantly affected by changes in brain states, either directly or via thalamic mode changes, certain features of cortical processing are consistent across various brain states, including anesthesia; these processing features include functional circuitry

within thalamic and cortical networks, principles of coding of external stimuli by individual neurons, and cycle-to-cycle dynamics of stimulus-driven responses and of motor outputs (Ahissar and Vaadia 1990; Simons et al. 1992; Ahissar et al. 1998; Worgotter et al. 1998; Vanderwolf 2000; Ego-Stengel et al. 2001; Sosnik et al. 2001; Bahar et al. 2004; Chen et al. 2007; Horwitz et al. 2007; King et al. 2007; Knutsen et al. 2008; Walker et al. 2008; Curto et al. 2009; Hromadka and Zador 2009; Huetz et al. 2011). Importantly, these features are consistent across states not only in the vibrissal system but in other modalities as well.

Obviously, studying the coding of whisker motion and touch in an awake state and based on natural whisking could yield conclusions that are different from those presented here. However, taking together peripheral and central effects of anesthesia and artificial whisking, as described above, suggests that such differences would be primarily related to the magnitude of response variables and not to coding principles.

Relevance to Behaving Rodents

Differences in neuronal states between different behavioral modes (e.g., quiescent, attentive, alert, exploring, whisking, and palpating) are not smaller than the difference between each of these modes and the anesthesia mode (Ahissar and Vaadia 1990; Fanselow and Nicolelis 1999; Castro-Alamancos 2002; Ferezou et al. 2006; Frostig 2006; Lee et al. 2008; Poulet and Petersen 2008; Crochet et al. 2011). Thus, questions about the relevance of findings in one mode to processing in another mode are valid in all these cases. While data from behaving rodents are still sparse, the consistencies described above are encouraging for postulating that findings related to coding and dynamics in anesthetized preparations are relevant to at least several behaving modes.

Specifically, several of our observations with artificial whisking in anesthetized rats are consistent with parallel observations in behaving rodents (Table 2). One such consistency, between the interlaminar activity ratios and firing distributions observed in our anesthetized rats and those observed in behaving mice (O'Connor, Peron et al. 2010), is depicted in Supplementary Figure 1; despite an overall ~2-fold reduction in activity levels, activity ratios and firing distributions across cortical layers were similar in the 2 cases. It should be mentioned, though, that some recordings in awake rats seem to reflect substantial differences from those in anesthetized ones. Those however should be compared with cautious. For example, recordings based on EMG of pad muscles as indicators of whisking dynamics often show low modulations of neuronal responses to whisking in air (e.g., Curtis and Kleinfeld 2009). Such low modulation rates, however, can be explained by the limited ability of EMG signals to accurately predict whisker motion. As sensory signals are locked to whisker motion, and not to EMG signals, this may decrease the measured correlation between the two.

Overall, our results from artificial whisking in anesthetized rats indicate that the thalamocortical system is capable of generating neuronal representations of object position using several coding schemes that work in parallel. Which of these coding schemes is used, or emphasized, in a given behavioral context is a subject for further studies.

Closed Versus Open Loop Thalamocortical Processing

Our thalamocortical neurons exhibited several codes to represent object location. While transformations between these codes at SS may employ local feed-forward computations (e.g., phase detection in thalamus or S1L4 and threshold in S1L23), the dynamics of their convergence and the existence of history-dependent mechanisms suggest that the collective computation scheme of the thalamocortical network is based on repetitive iterations in closed-loops. As a result, position codes reliability increases from cycle to cycle until stabilized (Fig. 6). Determination of whether these dynamics reflect a convergence mechanism that is dominated by re-entrant processes between separate neuronal stations (Edelman 1993), by a relaxation process within a homogeneous neural network (Hopfield 1982; Chakrabarti and Basu 2008), or by iterative processes in nested loops (Tweed 2003), requires further investigation.

Convergence dynamics allow a gradual decrease of perceptual error, regardless of the nature of the underlying mechanism. With convergence, perceptual decision times are a direct and simple function of perceptual confidence, where higher confidence levels entail delayed decision times (Saig et al. 2012). The parallel existence of several valid representations in the thalamocortical network allows for a flexible context-dependent selection process. The motor-sensory convergence strategy can use either of these thalamocortical representations as its primary internal

Table 2
Consistencies with recordings from behaving rodents

#	Our study	Recordings from behaving rodents
1	T&R representations observed mainly in S1L4, S2L46 and in VPM (Fig. 6).	T&R representations mainly in S1L4 (Curtis and Kleinfeld 2009) (Thalamic and S2 cells were not recorded).
2	Highly discriminative LL coding neurons observed in S1L23 (Fig. 6).	A sparse population of highly discriminative neurons is present in S1L23 of mice performing azimuthal object localization (O'Connor, Peron, et al. 2010).
3	Thalamocortical convergence occurs in ~4 cycles. (Figs 2, 3, 6, and 8).	Behavioral convergence occurs in ~4 cycles. (Knutsen et al. 2006; Horev et al. 2011).
4	Responses in the barrel cortex are modulated during active touch in a layer-specific manner (Figs 4–6).	Responses in the barrel cortex are modulated during active touch in a layer-specific manner (Krupa et al. 2004).
5	Responses in S1L23 are weaker than those in deeper layers (Fig. 7).	Responses in S1L23 are weaker than those in deeper layers in both awake rats and mice (de Kock and Sakmann 2009; O'Connor, Peron, et al. 2010).
6	Whisking in air induces significant modulations in thalamic and cortical neurons (Fig. 2).	Whisking in air induces significant modulations in thalamic and cortical neurons as is evident directly from spike activity (de Kock and Sakmann 2009; O'Connor, Peron, et al. 2010), and indirectly from fluctuations in membrane potentials of S1L23 cells (Crochet and Petersen 2006; Poulet and Petersen 2008), cells which receive mostly cortical-inputs (Feldmeyer et al. 2002; Bureau et al. 2006; Schubert et al. 2007).
7	The effect of active touch is mainly excitatory, although inhibitory effects are occasionally observed (Figs 3–5).	The effect of active touch is mainly excitatory (Krupa et al. 2004; Crochet and Petersen 2006; Poulet and Petersen 2008; Curtis and Kleinfeld 2009; O'Connor, Peron, et al. 2010), although inhibitory effects are occasionally observed in both modes (Krupa et al. 2004; Yu et al. 2006).

representation and base its global convergence dynamics on the accumulated confidence level of the selected representation. In this way, thalamocortical spike-count code may be used along with a restricted whisking range when a restricted search paradigm is required (O'Connor et al. 2013), and thalamocortical T&R code may be used along with nonrestricted whisking when object location is required to be translated to head coordinates (Curtis and Kleinfeld 2009). The selection of appropriate thalamocortical representation along with an appropriate motor-sensory strategy can be achieved during development (Gordon and Ahissar 2012; Gordon et al. 2013).

Supplementary Material

Supplementary material can be found at: http://www.cercor.oxfordjournals.org/

Funding

This work was supported by the Israel Science Foundation grant #749/10, Sir David Alliance CBE and the United States-Israel Bi-national Science Foundation grant #2011432.

Notes

We thank Dr Knarik Bagdasarian for invaluable experimental support, Mathew Diamond, David Kleinfeld, Avraham Saig, and Inbar Saraf-Sinik for enlightening discussions and comments on the manuscript, and Dr Barbara Schick for reviewing the article. Author Contributions: C.Y., D.D., and E.A. conceived and designed the project. C.Y. and D.D. conducted the experiments. C.Y., G.H., N.R., and E.A. analyzed the data. S.H. conducted the histological analysis. G.H. and N.R. provided analytical tools. C.Y., G.H., and E.A. wrote the manuscript. *Conflict of Interest:* E.A. holds the Helen Diller Family Chair in Neurobiology.

REFERENCES

Adibi M, McDonald JS, Clifford CW, Arabzadeh E. 2013. Adaptation improves neural coding efficiency despite increasing correlations in variability. J Neurosci. 33:2108–2120.

Agmon A, Connors BW. 1992. Correlation between intrinsic firing patterns and thalamocortical synaptic responses of neurons in mouse barrel cortex. J Neurosci. 12:319–329.

Ahissar E. 1998. Temporal-code to rate-code conversion by neuronal phase-locked loops. Neural Comput. 10:597–650.

Ahissar E, Abeles M, Ahissar M, Haidarliu S, Vaadia E. 1998. Hebbian-like functional plasticity in the auditory cortex of the behaving monkey. Neuropharmacol. 37:633–655.

Ahissar E, Knutsen PM. 2008. Object localization with whiskers. Biol Cybern. 98:449–458.

Ahissar E, Sosnik R, Bagdasarian K, Haidarliu S. 2001. Temporal frequency of whisker movement. II. Laminar organization of cortical representations. J Neurophysiol. 86:354–367.

Ahissar E, Sosnik R, Haidarliu S. 2000. Transformation from temporal to rate coding in a somatosensory thalamocortical pathway. Nature. 406:302–306.

Ahissar E, Vaadia E. 1990. Oscillatory activity of single units in a somatosensory cortex of an awake monkey and their possible role in texture analysis. Proc Natl Acad Sci USA. 87:8935–8939.

Alloway KD, Hoffer ZS, Hoover JE. 2003. Quantitative comparisons of corticothalamic topography within the ventrobasal complex and the posterior nucleus of the rodent thalamus. Brain Res. 968:54–68.

Alloway KD, Mutic JJ, Hoffer ZS, Hoover JE. 2000. Overlapping corticostriatal projections from the rodent vibrissal representations in primary and secondary somatosensory cortex. J Comp Neurol. 428:51–67.

Alloway KD, Roy SA. 2002. Conditional cross-correlation analysis of thalamocortical neurotransmission. Behav Brain Res. 135:191–196.

Angel A, Berridge DA, Unwin J. 1973. The effect of anaesthetic agents on primary cortical evoked responses. Br J Anaesth. 45:824–836.

Angel A, Unwin J. 1970. The effect of urethane on transmission along the dorsal column sensory pathway in the rat. J Physiol. 208:32P–33P.

Arabzadeh E, Zorzin E, Diamond ME. 2005. Neuronal encoding of texture in the whisker sensory pathway. PLoS Biol. 3:e17.

Bagdasarian K, Szwed M, Knutsen PM, Deutsch D, Derdikman D, Pietr M, Simony E, Ahissar E. 2013. Pre-neuronal morphological processing of object location by individual whiskers. Nat Neurosci. 16:622–631.

Bahar A, Dudai Y, Ahissar E. 2004. Neural signature of taste familiarity in the gustatory cortex of the freely behaving rat. J Neurophysiol. 92:3298–3308.

Bale MR, Petersen RS. 2009. Transformation in the neural code for whisker deflection direction along the lemniscal pathway. J Neurophysiol. 102:2771–2780.

Benjamini Y, Hochberg Y. 1995. Controlling the false discovery rate—a practical and powerful approach to multiple testing. J Roy Stat Soc B. 57:289–300.

Benjamini Y, Krieger AM, Yekutieli D. 2006. Adaptive linear step-up procedures that control the false discovery rate. Biometrika. 93:491–507.

Berg RW, Kleinfeld D. 2003. Rhythmic whisking by rat: retraction as well as protraction of the vibrissae is under active muscular control. J Neurophysiol. 89:104–117.

Birdwell JA, Solomon JH, Thajchayapong M, Taylor MA, Cheely M, Towal RB, Conradt J, Hartmann MJ. 2007. Biomechanical models for radial distance detection by rat vibrissae. J Neurophysiol. 98:2439–2455.

Bokor H, Acsady L, Deschenes M. 2008. Vibrissal responses of thalamic cells that project to the septal columns of the barrel cortex and to the second somatosensory area. J Neurosci. 28:5169–5177.

Bokor H, Frere SG, Eyre MD, Slezia A, Ulbert I, Luthi A, Acsady L. 2005. Selective GABAergic control of higher-order thalamic relays. Neuron. 45:929–940.

Bosman LW, Houweling AR, Owens CB, Tanke N, Shevchouk OT, Rahmati N, Teunissen WH, Ju C, Gong W, Koekkoek SK et al. 2011. Anatomical pathways involved in generating and sensing rhythmic whisker movements. Front Integr Neurosci. 5:53.

Bourassa J, Pinault D, Deschenes M. 1995. Corticothalamic projections from the cortical barrel field to the somatosensory thalamus in rats: a single-fibre study using biocytin as an anterograde tracer. Eur J Neurosci. 7:19–30.

Brecht M. 2007. Barrel cortex and whisker-mediated behaviors. Curr Opin Neurobiol. 17:408–416.

Bruno RM, Khatri V, Land PW, Simons DJ. 2003. Thalamocortical angular tuning domains within individual barrels of rat somatosensory cortex. J Neurosci. 23:9565–9574.

Bruno RM, Sakmann B. 2006. Cortex is driven by weak but synchronously active thalamocortical synapses. Science. 312:1622–1627.

Bureau I, von Saint Paul F, Svoboda K. 2006. Interdigitated paralemniscal and lemniscal pathways in the mouse barrel cortex. PLoS Biol. 4:e382.

Carvell GE, Simons DJ. 1987. Thalamic and corticocortical connections of the second somatic sensory area of the mouse. J Comp Neurol. 265:409–427.

Castro-Alamancos MA. 2002. Role of thalamocortical sensory suppression during arousal: focusing sensory inputs in neocortex. J Neurosci. 22:9651–9655.

Castro-Alamancos MA. 2004. Dynamics of sensory thalamocortical synaptic networks during information processing states. Prog Neurobiol. 74:213–247.

Castro-Alamancos MA, Calcagnotto ME. 2001. High-pass filtering of corticothalamic activity by neuromodulators released in the thalamus during arousal: in vitro and in vivo. J Neurophysiol. 85:1489–1497.

Chakrabarti BK, Basu A. 2008. Neural network modeling. Prog Brain Res. 168:155–168.

Chen X, Han F, Poo MM, Dan Y. 2007. Excitatory and suppressive receptive field subunits in awake monkey primary visual cortex (V1). Proc Natl Acad Sci U S A. 104:19120–19125.

Chiel HJ, Ting LH, Ekeberg O, Hartmann MJ. 2009. The brain in its body: motor control and sensing in a biomechanical context. J Neurosci. 29:12807–12814.

Chmielowska J, Carvell GE, Simons DJ. 1989. Spatial organization of thalamocortical and corticothalamic projection systems in the rat SmI barrel cortex. J Comp Neurol. 285:325–338.
Crochet S, Petersen CC. 2006. Correlating whisker behavior with membrane potential in barrel cortex of awake mice. Nat Neurosci. 9:608–610.
Crochet S, Poulet JF, Kremer Y, Petersen CC. 2011. Synaptic mechanisms underlying sparse coding of active touch. Neuron. 69:1160–1175.
Curtis JC, Kleinfeld D. 2009. Phase-to-rate transformations encode touch in cortical neurons of a scanning sensorimotor system. Nat Neurosci. 12:492–501.
Curto C, Sakata S, Marguet S, Itskov V, Harris KD. 2009. A simple model of cortical dynamics explains variability and state dependence of sensory responses in urethane-anesthetized auditory cortex. J Neurosci. 29:10600–10612.
de Kock CP, Sakmann B. 2009. Spiking in primary somatosensory cortex during natural whisking in awake head-restrained rats is cell-type specific. Proc Natl Acad Sci U S A. 106:16446–16450.
Derdikman D, Yu C, Haidarliu S, Bagdasarian K, Arieli A, Ahissar E. 2006. Layer-specific touch-dependent facilitation and depression in the somatosensory cortex during active whisking. J Neurosci. 26:9538–9547.
Deschenes M, Bourassa J, Pinault D. 1994. Corticothalamic projections from layer V cells in rat are collaterals of long-range corticofugal axons. Brain Res. 664:215–219.
Deutsch D, Pietr M, Knutsen PM, Ahissar E, Schneidman E. 2012. Fast feedback in active sensing: touch-induced changes to whisker-object interaction. PLoS ONE. 7:e44272.
Diamond ME, von Heimendahl M, Knutsen PM, Kleinfeld D, Ahissar E. 2008. 'Where' and 'what' in the whisker sensorimotor system. Nat Rev Neurosci. 9:601–612.
Edelman GM. 1993. Neural Darwinism: selection and reentrant signaling in higher brain function. Neuron. 10:115–125.
Ego-Stengel V, Shulz DE, Haidarliu S, Sosnik R, Ahissar E. 2001. Acetylcholine-dependent induction and expression of functional plasticity in the barrel cortex of the adult rat. J Neurophysiol. 86:422–437.
Fanselow EE, Nicolelis MA. 1999. Behavioral modulation of tactile responses in the rat somatosensory system. J Neurosci. 19:7603–7616.
Feldmeyer D, Lubke J, Silver RA, Sakmann B. 2002. Synaptic connections between layer 4 spiny neurone-layer 2/3 pyramidal cell pairs in juvenile rat barrel cortex: physiology and anatomy of interlaminar signalling within a cortical column. J Physiol. 538:803–822.
Ferezou I, Bolea S, Petersen CC. 2006. Visualizing the cortical representation of whisker touch: voltage-sensitive dye imaging in freely moving mice. Neuron. 50:617–629.
Frostig RD. 2006. Functional organization and plasticity in the adult rat barrel cortex: moving out-of-the-box. Curr Opin Neurobiol. 16:445–450.
Fundin BT, Pfaller K, Rice FL. 1997. Different distributions of the sensory and autonomic innervation among the microvasculature of the rat mystacial pad. J Comp Neurol. 389:545–568.
Furuta T, Timofeeva E, Nakamura K, Okamoto-Furuta K, Togo M, Kaneko T, Deschenes M. 2008. Inhibitory gating of vibrissal inputs in the brainstem. J Neurosci. 28:1789–1797.
Gentet LJ, Avermann M, Matyas F, Staiger JF, Petersen CC. 2010. Membrane potential dynamics of GABAergic neurons in the barrel cortex of behaving mice. Neuron. 65:422–435.
Ghazanfar AA, Nicolelis MA. 2001. Feature article: the structure and function of dynamic cortical and thalamic receptive fields. Cereb Cortex. 11:183–193.
Gil Z, Connors BW, Amitai Y. 1999. Efficacy of thalamocortical and intracortical synaptic connections: quanta, innervation, and reliability [see comments]. Neuron. 23:385–397.
Golomb D, Ahissar E, Kleinfeld D. 2006. Coding of stimulus frequency by latency in thalamic networks through the interplay of GABAB-mediated feedback and stimulus shape. J Neurophysiol. 95:1735–1750.
Gordon G, Ahissar E. 2012. Hierarchical curiosity loops and active sensing. Neural Netw. 32:119–129.
Gordon G, Dorfman N, Ahissar E. 2013. Reinforcement active learning in the vibrissae system: optimal object localization. J Physiol Paris. 107:107–115.
Gottschaldt KM, Iggo A, Young DW. 1973. Functional characteristics of mechanoreceptors in sinus hair follicles of the cat. J Physiol. 235:287–315.
Greenberg DS, Houweling AR, Kerr JN. 2008. Population imaging of ongoing neuronal activity in the visual cortex of awake rats. Nat Neurosci. 11:749–751.
Groh A, Bokor H, Mease RA, Plattner VM, Hangya B, Stroh A, Deschenes M, Acsády L. 2014. Convergence of cortical and sensory driver inputs on single thalamocortical cells. Cerebral Cortex. 24:3167–3179.
Groh A, de Kock CP, Wimmer VC, Sakmann B, Kuner T. 2008. Driver or coincidence detector: modal switch of a corticothalamic giant synapse controlled by spontaneous activity and short-term depression. J Neurosci. 28:9652–9663.
Guillery RW, Sherman SM. 2002. Thalamic relay functions and their role in corticocortical communication: generalizations from the visual system. Neuron. 33:163–175.
Helmstaedter M, Sakmann B, Feldmeyer D. 2009. Neuronal correlates of local, lateral, and translaminar inhibition with reference to cortical columns. Cereb Cortex. 19:926–937.
Hill DN, Bermejo R, Zeigler HP, Kleinfeld D. 2008. Biomechanics of the vibrissa motor plant in rat: rhythmic whisking consists of triphasic neuromuscular activity. J Neurosci. 28:3438–3455.
Hoogland PV, Welker E, Van der Loos H. 1987. Organization of the projections from barrel cortex to thalamus in mice studied with Phaseolus vulgaris-leucoagglutinin and HRP. Exp Brain Res. 68:73–87.
Hopfield JJ. 1982. Neural networks and physical systems with emergent selective computational abilities. Proc Natl Acad Sci USA. 79:2554–2558.
Horev G, Saig A, Knutsen PM, Pietr M, Yu C, Ahissar E. 2011. Motor-sensory convergence in object localization: a comparative study in rats and humans. Philos Trans R Soc Lond Ser B Biol Sci. 366:3070–3076.
Horwitz GD, Chichilnisky EJ, Albright TD. 2007. Cone inputs to simple and complex cells in V1 of awake macaque. J Neurophysiol. 97:3070–3081.
Hromadka T, Zador AM. 2009. Representations in auditory cortex. Curr Opin Neurobiol. 19:430–433.
Huetz C, Gourevitch B, Edeline JM. 2011. Neural codes in the thalamocortical auditory system: from artificial stimuli to communication sounds. Hear Res. 271:147–158.
Jeffress LA. 1948. A place theory of sound localization. J Comp Physiol Psychol. 41:35–39.
King AJ, Bajo VM, Bizley JK, Campbell RA, Nodal FR, Schulz AL, Schnupp JW. 2007. Physiological and behavioral studies of spatial coding in the auditory cortex. Hear Res. 229:106–115.
Kleinfeld D, Ahissar E, Diamond ME. 2006. Active sensation: insights from the rodent vibrissa sensorimotor system. Curr Opin Neurobiol. 16:435–444.
Knutsen PM, Ahissar E. 2009. Orthogonal coding of object location. Trends Neurosci. 32:101–109.
Knutsen PM, Biess A, Ahissar E. 2008. Vibrissal kinematics in 3D: tight coupling of azimuth, elevation, and torsion across different whisking modes. Neuron. 59:35–42.
Knutsen PM, Derdikman D, Ahissar E. 2005. Tracking whisker and head movements in unrestrained behaving rodents. J Neurophysiol. 93:2294–2301.
Knutsen PM, Pietr M, Ahissar E. 2006. Haptic object localization in the vibrissal system: behavior and performance. J Neurosci. 26:8451–8464.
Koralek KA, Jensen KF, Killackey HP. 1988. Evidence for two complementary patterns of thalamic input to the rat somatosensory cortex. Brain Res. 463:346–351.
Krupa DJ, Wiest MC, Shuler MG, Laubach M, Nicolelis MA. 2004. Layer-specific somatosensory cortical activation during active tactile discrimination. Science. 304:1989–1992.
Lee S, Carvell GE, Simons DJ. 2008. Motor modulation of afferent somatosensory circuits. Nat Neurosci. 11:1430–1438.
Leiser SC, Moxon KA. 2007. Responses of trigeminal ganglion neurons during natural whisking behaviors in the awake rat. Neuron. 53:117–133.
Lottem E, Azouz R. 2008. Dynamic translation of surface coarseness into whisker vibrations. J Neurophysiol. 100:2852–2865.
Lottem E, Azouz R. 2009. Mechanisms of tactile information transmission through whisker vibrations. J Neurosci. 29:11686–11697.

Lu SM, Lin RC. 1993. Thalamic afferents of the rat barrel cortex: a light- and electron-microscopic study using Phaseolus vulgaris leucoagglutinin as an anterograde tracer. Somatosens Mot Res. 10:1–16.
Maggi CA, Meli A. 1986. Suitability of urethane anesthesia for physiopharmacological investigations. Part 3: other systems and conclusions. Experientia. 42:531–537.
Maravall M, Petersen RS, Fairhall AL, Arabzadeh E, Diamond ME. 2007. Shifts in coding properties and maintenance of information transmission during adaptation in barrel cortex. PLoS Biol. 5:e19.
McCormick DA, von Krosigk M. 1992. Corticothalamic activation modulates thalamic firing through glutamate "metabotropic" receptors. Proc Natl Acad Sci USA. 89:2774–2778.
Mitchinson B, Gurney KN, Redgrave P, Melhuish C, Pipe AG, Pearson M, Gilhespy I, Prescott TJ. 2004. Empirically inspired simulated electro-mechanical model of the rat mystacial follicle-sinus complex. Proc Biol Sci. 271:2509–2516.
Mitchinson B, Martin CJ, Grant RA, Prescott TJ. 2007. Feedback control in active sensing: rat exploratory whisking is modulated by environmental contact. Proc Biol Sci. 274:1035–1041.
Nguyen QT, Kleinfeld D. 2005. Positive feedback in a brainstem tactile sensorimotor loop. Neuron. 45:447–457.
Nicolelis MA, Fanselow EE. 2002. Thalamocortical optimization of tactile processing according to behavioral state. Nat Neurosci. 5:517–523.
O'Connor DH, Clack NG, Huber D, Komiyama T, Myers EW, Svoboda K. 2010. Vibrissa-based object localization in head-fixed mice. J Neurosci. 30:1947–1967.
O'Connor DH, Hires SA, Guo ZV, Li N, Yu J, Sun Q-Q, Huber D, Svoboda K. 2013. Neural coding during active somatosensation revealed using illusory touch. Nat Neurosci. 16:958–965.
O'Connor DH, Peron SP, Huber D, Svoboda K. 2010. Neural activity in barrel cortex underlying vibrissa-based object localization in mice. Neuron. 67:1048–1061.
Okun M, Lampl I. 2008. Instantaneous correlation of excitation and inhibition during ongoing and sensory-evoked activities. Nat Neurosci. 11:535–537.
Petersen RS, Panzeri S, Maravall M. 2009. Neural coding and contextual influences in the whisker system. Biol Cybern. 100:427–446.
Pierret T, Lavallee P, Deschenes M. 2000. Parallel streams for the relay of vibrissal information through thalamic barreloids. J Neurosci. 20:7455–7462.
Poulet JF, Petersen CC. 2008. Internal brain state regulates membrane potential synchrony in barrel cortex of behaving mice. Nature. 454:881–885.
Quist BW, Hartmann MJ. 2012. Mechanical signals at the base of a rat vibrissa: the effect of intrinsic vibrissa curvature and implications for tactile exploration. J Neurophysiol. 107:2298–2312.
Ramcharan E, Gnadt J, Sherman S. 2005. Higher-order thalamic relays burst more than first-order relays. Proc Natl Acad Sci U S A. 102:12236–12241.
Ritt JT, Andermann ML, Moore CI. 2008. Embodied information processing: vibrissa mechanics and texture features shape micromotions in actively sensing rats. Neuron. 57:599–613.
Saig A, Gordon G, Assa E, Arieli A, Ahissar E. 2012. Motor-sensory confluence in tactile perception. J Neurosci. 32:14022–14032.
Schubert D, Kotter R, Staiger JF. 2007. Mapping functional connectivity in barrel-related columns reveals layer- and cell type-specific microcircuits. Brain Struct Funct. 212:107–119.
Sharp FR, Evans K. 1982. Regional (14C) 2-deoxyglucose uptake during vibrissae movements evoked by rat motor cortex stimulation. J Comp Neurol. 208:255–287.
Sherman SM, Guillery RW. 1996. Functional organization of thalamocortical relays. J Neurophysiol. 76:1367–1395.
Simons DJ, Carvell GE, Hershey AE, Bryant DP. 1992. Responses of barrel cortex neurons in awake rats and effects of urethane anesthesia. Exp Brain Res. 91:259–272.
Simony E, Bagdasarian K, Herfst L, Brecht M, Ahissar E, Golomb D. 2010. Temporal and spatial characteristics of vibrissa responses to motor commands. J Neurosci. 30:8935–8952.
Sosnik R, Haidarliu S, Ahissar E. 2001. Temporal frequency of whisker movement. I. Representations in brain stem and thalamus. J Neurophysiol. 86:339–353.
Stuttgen MC, Kullmann S, Schwarz C. 2008. Responses of rat trigeminal ganglion neurons to longitudinal whisker stimulation. J Neurophysiol. 100:1879–1884.
Swadlow HA. 2000. Descending corticofugal neurons in layer 5 of rabbit S1: evidence for potent corticocortical, but not thalamocortical, input. Exp Brain Res. 130:188–194.
Szwed M, Bagdasarian K, Ahissar E. 2003. Encoding of vibrissal active touch. Neuron. 40:621–630.
Towal RB, Hartmann MJ. 2006. Right-left asymmetries in the whisking behavior of rats anticipate head movements. J Neurosci. 26:8838–8846.
Towal RB, Hartmann MJ. 2008. Variability in velocity profiles during free-air whisking behavior of unrestrained rats. J Neurophysiol. 100:740–752.
Tweed D. 2003. Microcosms of the brain: what sensorimotor systems reveal about the mind. Oxford: Oxford University Press.
Urbain N, Deschenes M. 2007. A new thalamic pathway of vibrissal information modulated by the motor cortex. J Neurosci. 27:12407–12412.
Vanderwolf CH. 2000. Are neocortical gamma waves related to consciousness? Brain Res. 855:217–224.
Venkatraman S, Carmena J. 2011. Active sensing of target location encoded by cortical microstimulation. IEEE Trans Neural Syst Rehabil Eng. 19:317–324.
Walker KM, Ahmed B, Schnupp JW. 2008. Linking cortical spike pattern codes to auditory perception. J Cogn Neurosci. 20:135–152.
Wang Q, Webber RM, Stanley GB. 2010. Thalamic synchrony and the adaptive gating of information flow to cortex. Nat Neurosci. 13:1534–1541.
White EL, Keller A. 1987. Intrinsic circuitry involving the local axon collaterals of corticothalamic projection cells in mouse SmI cortex. J Comp Neurol. 262:13–26.
Worgotter F, Suder K, Zhao Y, Kerscher N, Eysel UT, Funke K. 1998. State-dependent receptive-field restructuring in the visual cortex. Nature. 396:165–168.
Yu C, Derdikman D, Haidarliu S, Ahissar E. 2006. Parallel Thalamic Pathways for Whisking and Touch Signals in the Rat. PLoS Biol. 4: e124.
Zucker E, Welker WI. 1969. Coding of somatic sensory input by vibrissae neurons in the rat's trigeminal ganglion. Brain Res. 12:138–156.